Barrier Penetration Effects for Light Nuclei*†

B. E. FREEMAN‡ AND J. L. MCHALE
Yale University, New Haven, Connecticut

(Received August 11, 1952)

The penetration parameters F_L^2/ρ, ρ/G_L^2, and ρ/A_L^2 have been compared as functions of energy for a number of reactions induced by proton or alpha-particle bombardment of light nuclei. It was found that these parameters behaved quite similarly in the energy range considered, particularly for $L>0$. The limitations on the applicability of barrier "penetration factors" in the treatment of reaction cross sections are investigated by computing a number of typical cases, making use of the one-body model with allowance for absorption of the incident wave. Several sets of values of nuclear radius and well depth were used. The relation between the one-body cross section without absorption and the channel penetration parameters, f_L^2/ρ and ρ/g_L^2, is treated in some detail for the $Li^7(p,\alpha)\alpha$ reaction. Breit's consideration of the case of very strong absorption $\sigma_L \propto 1/A_L^2$, is also presented. The connection between the one-body model without absorption and a one-level dispersion formula in the vicinity of sharp resonance is used to tabulate the properties of a number of one-body resonances. In a number of cases resonances were found to be broadened markedly by the absorption of the incident wave in nuclear matter.

I. INTRODUCTION

IN the past, "penetration factors" have been applied extensively to study nuclear reactions involving the absorption or emission of charged particles. Such a factorization is supposed to split off the barrier dependence of the damping constant Γ which characterizes the prescribed disintegration channel. The residual factor contained in Γ is then to depend only on the behavior of the compound nucleus in releasing disintegration products in the absence of the barrier.

With the exception of certain limiting cases, however, this procedure is incompatible with evidence obtained on the basis of simplified models of the nucleus. In the general case it is found that barrier effects cannot be separated from those of specifically nuclear origin. Excitation functions calculated for such models provide a useful measure of barrier penetration and resonance effects, but it is not intended to substitute them for more complete considerations of many-body features of the reactions.

Various combinations of the regular and irregular Coulomb functions, F_L and G_L, evaluated at the nuclear surface, have been proposed as penetration parameters. The form $\Gamma \propto F_L^2/\rho$ is perhaps the most widely employed penetration parameter. As will be seen later, it represents a limiting case of the one-body model of the nucleus. Konopinski and Bethe[1] used the relation $\Gamma \propto \rho/G_L^2$, suggested by Kapur and Peierls,[2] to study several reactions with light nuclei. Christy and Latter,[3] guided by the considerations of Wigner[4] and Wigner and Eisenbud,[5] applied the penetration parameter ρ/A_L^2 to the study of a number of reactions with light elements. The damping constant Γ is also expressible in terms of the quantities f_L^2/ρ or ρ/g_L^2 under special conditions. Here, $f_L=F_L\cos K_L+G_L\sin K_L$ and $g_L=G_L\cos K_L-F_L\sin K_L$ are Coulomb functions corrected for the presence of an average nuclear potential, which produces a phase shift K_L. Breit[6] obtained the relation $\Gamma \propto f_L^2/\rho$ for a weakly coupled resonating nuclear element under the idealization of sharp localization in space; a similar result is obtained in his schematic treatment of nuclear resonances.[7] For a strong repulsive interaction in a large region, however, the result $\Gamma \propto \rho/g_L^2$ is obtained. The reason for considering all these possibilities is that for different nuclear models one or another penetration parameter can be used in a simple formula. The parameters listed above apply to limiting cases of the more general conditions determined by the location of resonating elements in the compound nucleus, the competition from other channels, and other factors.

The publication of extended tables of the Coulomb functions[8] eliminates the uncertain and possibly large errors introduced by the employment of the J.W.B.K. approximation to the square of the Coulomb functions. But the absence of a unique definition of a penetration parameter emphasizes the uncertainties and need for caution in the application of "penetration factors."

In some cases, such as the escape of α-particles from radioactive nuclei, the main interest has been in the approximate energy dependence of the mean life. Here it does not matter much how the barrier penetration effects are treated, nearly equivalent results being obtained by different methods. For light nuclei, however, one can obtain appreciable differences depending on which of the current conventions is used. The main

* Part of a dissertation submitted by Burton E. Freeman for the degree of Doctor of Philosophy at Yale University.

† Assisted by the joint program of the ONR and AEC.

‡ Now at the Los Alamos Scientific Laboratory, Los Alamos, New Mexico.

[1] E. J. Konopinski and H. A. Bethe, Phys. Rev. **54**, 130 (1938).

[2] P. R. Kapur and R. Peierls, Proc. Roy. Soc. (London) **A166**, 277 (1938).

[3] R. F. Christy and R. Latter, Revs. Modern Phys. **20**, 185 (1948).

[4] E. P. Wigner, Phys. Rev. **70**, 15 (1946); Phys. Rev. **70**, 606 (1946).

[5] E. P. Wigner and L. Eisenbud, Phys. Rev. **72**, 29 (1947).

[6] G. Breit, Phys. Rev. **58**, 506 (1940).

[7] G. Breit, Phys. Rev. **69**, 472 (1946).

[8] Bloch, Hull, Broyles, Bouricius, Freeman, and Breit, Revs. Modern Phys. **23**, 147 (1951).

distinction between these problems is the fact that in studies of reactions of the lighter nuclei one is concerned with relatively wide resonances and with the interpretation of yield *versus* bombarding energy data. A variation of a coefficient by a factor 2 or 4 can be of considerable interest if one tries to test different hypotheses regarding the location of virtual energy levels. Such problems did not arise in the work of Gamow[9] and of Condon and Gurney[10] on the original explanation of the Geiger-Nuttall relation. It has been shown by Ostrofsky, Breit, and Johnson[11] that the nuclear model used and the barrier effects can combine themselves in such a way that the simple application of a barrier "penetration factor" can be seriously in error. This fact is obvious through an inspection of their graphs which give very different yield curves depending on the model used.

In the present paper, the mutual consistency of the penetration parameters is tested, and their applicability is determined by computing theoretical yield-energy curves making use of simplifying assumptions somewhat similar to those of OBJ. Only one reaction is studied from the point of view of comparison with experiment. In other cases, the object is to enable an experimental worker to form a reasonably immediate judgment regarding the effect of a change in the model on the shape of the cross section-energy curve. In many cases below, the words "penetration parameter" are used in preference to "penetration factor" so as to emphasize the fact that a potential barrier affects the cross section in a somewhat more complicated manner than through the application of a factor. On the other hand, it will be seen that in some cases "penetration factors" give a good representation of the more accurate relations.

For the sake of simplicity, the calculations on the energy dependence of cross sections are confined to the one-body model, with the inclusion of effects of absorption of the incident wave. The phase shift K_L contained in the definition of f_L and g_L is therefore determined by a one-body approximation. The variety of situations covered has turned out to be so great that only a small fraction of the available material could be prepared for publication.[12] On the other hand, some of the penetration parameters studied below have a general significance also in a many-body approach as has been shown by Breit.[7] On the whole, the study indicates that less care has to be exercised regarding the choice of the penetration parameter when barrier effects are pronounced.

[9] G. Gamow, Physik. Z. **32**, 651 (1931); Z. Physik **52**, 510 (1929); Nature **122**, 805 (1929).
[10] E. U. Condon and R. U. Gurney, Phys. Rev. **33**, 127 (1929).
[11] Ostrofsky, Breit, and Johnson, Phys. Rev. **49**, 22 (1936). This paper is referred to as OBJ in the text.
[12] With the exception of certain representative cases, space limitations prevent the inclusion in this paper of the curves obtained. The unpublished plots can be procured from G. Breit, Sloane Physics Laboratory, Yale University, New Haven, Connecticut.

Notation and Symbols[8]

F_L=regular Coulomb function: $F_L \sim \sin(\rho - \frac{1}{2}L\pi - \eta(\ln 2\rho) + \sigma_L)$. G_L=irregular Coulomb function: $G_L \sim \cos(\rho - \frac{1}{2}L\pi - \eta(\ln 2\rho) + \sigma_L)$. A_L, φ_L=phase amplitude variables: $A_L = |F_L^2 + G_L^2|^{\frac{1}{2}}$ with $F_L = A_L \sin\varphi_L$ and $G_L = A_L \cos\varphi_L$; and $\varphi_L = 0$ when $\rho = 0$. $\rho = kr$, where r is the interparticle separation and $k = \mu v/\hbar = 2\pi/\Lambda$. The quantity μ is the reduced mass and v is the relative velocity of the colliding particles.

$\eta = ZZ'e^2/\hbar v$, where Z and Z' are the atomic numbers of the collision partners. $\mathfrak{F}_L$=solution of the one-body radial equation,

$$[d^2/dr^2 + (2\mu/\hbar^2)\{E' - V + (i\hbar/2)P - L(L+1)/r^2\}]\mathfrak{F}_L = 0.$$

$V(r)$ and $P(r)$ are real quantities such that $V(r) = ZZ'e^2/r$ and $P(r) = 0$ for $r > r_0$; r_0 is the radius of the compound nucleus; E' is the energy of relative motion. For $r > r_0$,

$$\mathfrak{F}_L = e^{iK_L}(F_L \cos K_L + G_L \sin K_L).$$

$$z^2 = (2\mu/\hbar^2)[E' - V + (i\hbar/2)P]r^2 = (k'r)^2 = (k_0' + ik_1')^2 r^2 = (\alpha + i\beta)$$

where k_0', k_1', α, and β are all real quantities. They satisfy

$$(2\mu/\hbar^2)(E' - V)r^2 = (k_0 r)^2 = (k_0' r)^2 - (k_1' r)^2 = \alpha,$$
$$(\mu/\hbar)Pr^2 = 2k_0' k_1' r^2 = \beta.$$

The symbol k_1' is called the absorption coefficient.

In the cross-section formulas, the following symbols and abbreviations are used:

σ_L=partial cross section for a reaction.
$\delta_L = dF_L/F_L d\rho - d\mathfrak{F}_L/\mathfrak{F}_L d\rho$;
$\rho\delta_L = (\rho dF_L)/(F_L d\rho) - (zd\mathfrak{F}_L/\mathfrak{F}_L dz)$.
$u_L = \mathfrak{F}_L(r)/\mathfrak{F}_L(r_0)$.
$s = \sin(2k_0'r)$; $c = \cos(2k_0'r)$; $sh = \sinh(2k_1'r)$; and $ch = \cosh(2k_1'r)$. The abbreviation Re stands for the real part; Im stands for the imaginary part.

Guide to Figures

The following symbols and abbreviations have been used to simplify the labeling of the figures:

E_{Mev}=energy of incident particle in Mev.
E'_{Mev}=relative energy of motion in Mev.
$U = |V|$ where V is the real part of the nuclear potential.
$k'_1 = 0$ denotes the case of vanishingly small absorption.
$\mathfrak{L}_1 = \log_{10}\Pi_1 = \log_{10}(F_L^2/\rho)$.
$\mathfrak{L}_2 = \log_{10}\Pi_2 = \log_{10}(\rho/G_L^2)$.
$\mathfrak{l}_1 = \log_{10}\pi_1 = \log_{10}(f_L^2/\rho)$.
$\mathfrak{l}_2 = \log_{10}\pi_2 = \log_{10}(\rho/g_L^2)$.
$\mathfrak{L} = \log_{10}[10^{39}(\sigma_L v/2\pi P)\ \text{cm}^3]$.
$\mathfrak{P} = \log_{10}[10^{39}(2L+1)r_0^3(F_L/\rho)^2\ \text{cm}^3]$.

Incident channels for proton and alpha-particle bombardment are designated by $Z^A(p,\ )$ and $Z^A(\alpha,\ )$, respectively, where Z^A is the target isotope.

II. SCOPE OF CALCULATION

Under simplifying assumptions discussed in a later section, reaction cross sections have been calculated for the following conditions: (a) Incident particle: proton or alpha-particle; (b) Target nucleus: the elements from lithium to silicon; (c) Energy: from 0.5 to 5.0 Mev; (d) Relative angular momentum: from $L=0$ to $L=4$. Although these target elements and energies present no difficulty for proton bombardment, certain combinations of element and energy must be omitted for alpha-particles. The target element Si is the heaviest element for which Coulomb functions are available[8] with incident alpha-particles. The calculations have been made for values of the nuclear radius, r_0, given by

$$r_0=CA^{\frac{1}{3}},\quad C=1.6\times10^{-13}\quad\text{or}\quad 2.1\times10^{-13}\text{ cm},\quad (1)$$

where A is the mass number of the compound nucleus. The smaller of the two values of C corresponds approximately to some of the nuclear data in conventional interpretations. The larger value was used for two reasons: (a) it was desired to ascertain the effect of a change in r_0; (b) when a nucleus is bombarded by deuterons one has, in general, a variety of processes taking place, starting with a typical Oppenheimer-Phillips transfer and ending with the formation of a compound nucleus; a somewhat intermediate stage consists in the formation of a compound nucleus having a loose structure, with the deuteron being attached to the main body of the bombarded nucleus through the tail of either the neutron or the proton wave function.

The masses of the target nucleus and incident particle were approximated as integral multiples of the proton mass. The Coulomb parameter[8] η, which is large at low energies, is slightly in error because of the latter approximation. This means that the calculations apply to slightly lower energies than intended. But even for alpha-particle bombardment, the correction is only 0.6 percent, an amount which is negligible in comparison with the uncertainties of the one-body model.

III. COMPARISON OF BARRIER PENETRATIONS

The parameters $\Pi_1=F_L^2/\rho$ and $\Pi_2=\rho/G_L^2$ have been calculated for the reactions of protons on Li^7, B^{11}, N^{14}, Ne^{20}, Mg^{24} and Si^{28}, and compared with the results obtained by Christy and Latter,[3] who used a form proportional to $\Pi_3=\rho/A_L^2$. In the low energy limit these forms become equivalent, since for this limit $F_LG_L\propto\rho$ and $F_L\ll G_L$. Therefore, all three reduce to the limiting form $\exp\{-2\pi\eta\}$. Since the principal energy dependence of the partial cross section σ_L is given by the factor $(1/v^2)e^{-2\pi\eta}$ at sufficiently low energies, $\sigma_L\propto\Gamma/E$ in the low energy limit.

For the six target elements employed, the parameters

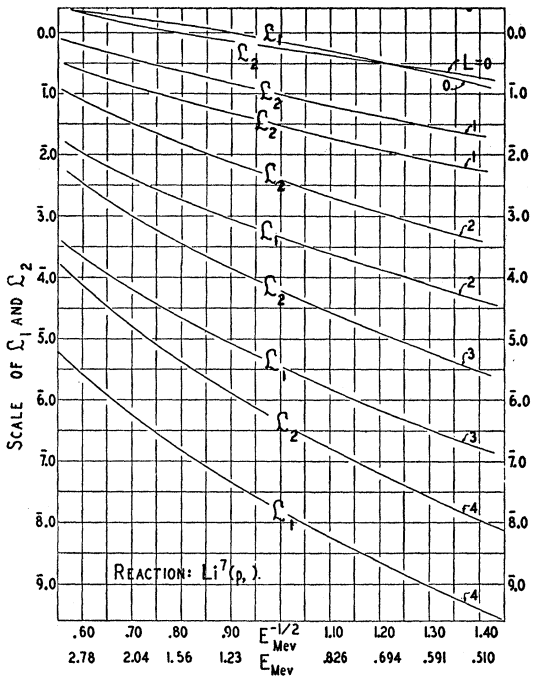

FIG. 1. Comparison of penetration parameters for $Li^7(p,\ )$: $\mathfrak{L}_1$ *vs* $E_{Mev}^{-\frac{1}{2}}$ and $\mathfrak{L}_2$ *vs* $E_{Mev}^{-\frac{1}{2}}$. The curves were normalized by fitting the $L=0$ pair at $E=3$ Mev. $r_0=1.6\times10^{-13}A^{\frac{1}{3}}$ cm.

Π_1 and Π_2 showed closely similar behavior as functions of energy. For large L the ratio Π_1/Π_2 is practically independent of energy in the range from $E=0.5$ to 3.0 Mev.

The comparison of Π_1 and Π_2 is illustrated[12] for proton bombardment of Li^7 in Fig. 1. It is seen that the curvatures of the two parameters differ markedly for $L=0$. For example, the Li^7 curves intersect at $E=0.62$ Mev when fitted at 3.0 Mev. The relative curvature of the $L=0$ parameters exhibited an interesting variation as a function of the atomic number Z' of the target nucleus. For Li^7, the curve ρ/G_0^2 is concave upward; this curvature decreases with increasing Z' until, for Si^{28}, it has reversed, and the curve for ρ/G_0^2 is everywhere above the F_0^2/ρ curve.

The curves[12] computed for the radius $r_0=2.1\times10^{-13}A^{\frac{1}{3}}$ cm agreed qualitatively with the results obtained for the smaller radius with minor exceptions. For example, using the same normalization employed for the smaller radius, the second intersection of Π_1 and Π_2 for $L=0$ is shifted to an energy less than 0.5 Mev.

Konopinski and Bethe[1] obtained a remarkable fit to the $Li^7(p,\alpha)\alpha$ experimental yield[13] up to $E=1$ Mev by assuming that $\Gamma\propto\Pi_2$ with $L=1$ and $r_0=1.65\times10^{-13}(A-1)^{\frac{1}{3}}$ cm. They also showed, in accordance with the selection rule corresponding to a spin $I=\frac{3}{2}$ and odd parity for the ground state of Li^7, that the data could not be fitted to a penetration parameter Π_2

[13] Rumbaugh, Roberts, and Hafstad, Phys. Rev. **54**, 657 (1938). Herb, Parkinson, and Kerst, Phys. Rev. **48**, 118 (1935).

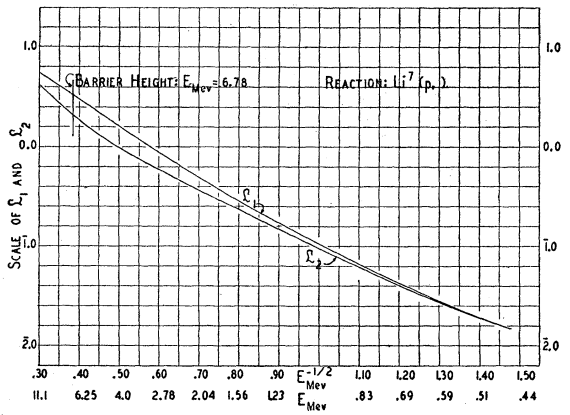

FIG. 2. Comparison of the penetration parameters F_1^2/ρ and G_1^2/ρ for $Li^7(p,\ )$ over an extended energy range: Ω_1 and Ω_2 *vs* $E_{Mev}^{-\frac{1}{2}}$ for $r_0=1.6\times10^{-13}A^{\frac{1}{3}}$ cm and $L=1$. The curves were fitted at 0.5 Mev.

with $L=0$. The results of the preceding paragraph indicate that their fit can be duplicated quite closely with a Π_1 parameter for $L=1$. In Fig. 2 these parameters are compared over an extended energy range. It is seen that the greatest disparity occurs roughly in the vicinity of the top of the potential barrier, $E=6.78$ Mev. The intersection phenomenon noted earlier for the $L=0$ case is apparently present here also, occurring off scale beyond $E=11$ Mev. In Sec. VI, the $Li^7(p,\alpha)\alpha$ reaction will be discussed on the basis of the one-body model of the nucleus.

Christy and Latter calculated Π_3 for protons incident on some light nuclei up to F^{19}, using the constant nuclear radius $e^2/mc^2\approx1.3\times10^{-13}$cm. A qualitative comparison of their curves from 0.5 to 3.0 Mev with those described here shows that they are similar functions of energy to within the estimated variation due to the different choice of radius. A more quantitative comparison is illustrated in Table I for $Li^7(p,\ )$ with $r_0=1.6\times10^{-13}A^{\frac{1}{3}}$ cm. For $L>1$ in the energy interval considered, the difference between A_L and G_L is completely negligible because of the high barrier and, thus, $\Pi_2=\Pi_3$. Since the minimum barrier occurs for $L=0$, the disparity between Π_2 and Π_3 is greatest here at a given energy. It is seen that $\Pi_2=\Pi_3$ in the $L=0$ case up to about 1 Mev, and $\Pi_2=\Pi_3$ up to about 2 Mev for $L=1$. In the latter case, moreover, the two parameters only differ by 3 percent at 3.0 Mev.

A comparison of the energy dependence of the penetration parameters with that of the collision cross section will be discussed later in connection with Fig. 6. The shape of the curve for parameter Γ_1 will be seen to be similar to that of the curve for the log of the yield calculated for a special choice of the potential energy well. An inspection of Figs. 1 and 3 of OBJ shows, however, that a considerable variation in the shapes of (σ, E) curves is obtained as a result of varying the assumed potential wells. If one wishes to determine the value of L from the experimental data one is confronted therefore with the necessity of eliminating the influence of these variations. While it is true that the data can be fitted by means of $L=1$, it is hardly possible to consider them as a proof that $L=1$. The actual situation does not consist in accounting for the data without a partial influence of resonance as might perhaps be concluded from a cursory examination of the paper of Konopinski and Bethe. It is also necessary to eliminate the variations in shape which can arise as a result of varying assumptions regarding the interactions inside the nucleus. These variations have been referred to in the OBJ paper in terms of a partial approach to resonance so as to correlate the curves more vividly with the assumed changes in potential wells. On the other hand, the assignment of $L=1$ to this reaction is highly probable as has been brought out by Breit[14] and by Konopinski and Bethe.[1] It has been pointed out by Breit in the same connection that the distinction between different values of L becomes artificial because one has to consider the possibility of perturbations from such configurations as p^2s and p^2d of the Li^7 nucleus which can react with incident s-particles without violation of the parity rule. The perturbations are considered to arise as a result of the incidence of the proton so that one has a compound nucleus in an even state even though one is dealing with an s-proton. For this reason the effect of the partial wave $L=0$ cannot be excluded by parity considerations alone and conclusions regarding which of the partial waves is dominant are more difficult than simple sticking probability considerations would lead one to believe.

An incident p-wave can cause the appearance of a perturbing configuration in a distant collision and the perturbing configuration can then interact with the s-wave. The energy dependences of distant p-wave collisions and close s-wave collisions are somewhat similar and an appreciable range of energies within which the two interactions can take place may be expected to exist. The $Li^7(p,\alpha)\alpha$ reaction will be discussed briefly again in connection with the work of Inglis and collaborators.[15]

IV. SUMMARY OF THE ONE-BODY MODEL

The calculations in the present paper are arranged along lines similar to those of Ostrofsky, Breit, and

TABLE I. Energy dependence of the penetration parameters Π_2 and Π_3 for $Li^7(p,\ )$ with $r_0=1.6\times10^{-13}A^{\frac{1}{3}}$ cm.

	$L=0$		$L=1$	
E	Π_2	Π_3	Π_2	Π_3
0.5	0.1806	0.1804	0.01844	0.01844
1.0	0.5227	0.5202	0.09604	0.09601
1.5	0.8761	0.7679	0.2106	0.2102
2.0	1.280	1.001	0.3545	0.3524
3.0	2.305	1.357	0.6560	0.6408

[14] G. Breit, Rev. Sci. Instr. **9**, 63 (1938).
[15] Heydenburg, Hudson, Inglis, and Whitehead, Phys. Rev. **73**, 241 (1948); Phys. Rev. **74**, 405 (1948); D. R. Inglis, Phys. Rev. **74**, 21 (1948).

Johnson, who made use of an absorption coefficient for the incident wave in the nuclear matter in order to account for the conversion of the wave from the incident channel to disintegration channels. The same device has been used later by Feshbach, Peaslee and Weisskopf[16] and by Serber *et al.*[17] It is realized that the formation of compound states owing their stability essentially to the participation of many nucleons is not taken account of in such a treatment. On the other hand, corrections for the formation of such states can be made in a number of ways as is well-known.

In the one-body model, the real potential $V(r)$ is replaced by the complex potential $V(r)-(i\hbar/2)P(r)$ for $r<r_0$. The introduction of a negative imaginary potential within the nuclear radius r_0 provides for absorption of particles from the beam at a rate $P|\Psi|^2$ per unit time per unit volume, where Ψ is the complete wave function, i.e., an incident plane wave of unit density modified by the Coulomb and nuclear potentials.

The partial reaction cross section without spin is obtained in the usual way. There results,

$$\sigma_L=(\Lambda^2/\pi v)(2L+1)|\mathfrak{F}_L(r_0)|^2\int_0^{r_0}P(r)|u_L|^2dr. \quad (2)$$

This formula differs from a corresponding one in OBJ only through the use of P which is a function of r rather than a constant. The formula can be expressed in terms of the wave function and its logarithmic derivative at the nuclear surface by noting that

$$\int_0^{r_0}P(r)|u_L|^2dr=-v\,\mathrm{Im}(d\mathfrak{F}_L/\mathfrak{F}_Ld\rho)_{r=r_0}. \quad (3)$$

Since at the nuclear surface $\mathfrak{F}_L$ must satisfy the usual one-body conditions[6]

$$\mathfrak{F}_L=F_L/[1-F_LG_L\delta_L-iF_L^2\delta_L], \quad (4)$$
$$\delta_L=dF_L/(F_Ld\rho)-d\mathfrak{F}_L/(\mathfrak{F}_Ld\rho),$$

the partial reaction cross section can be written as

$$\sigma_L=(\Lambda^2/\pi)(2L+1)\{(F_L^2\,\mathrm{Im}\delta_L)/|1-F_LG_L\delta_L-iF_L^2\delta_L|^2\}, \quad (5)$$

an equation which can be derived by an application of Green's theorem in a well-known manner. Since the cross section must vanish when P vanishes, $\mathrm{Im}\delta_L$ is different from zero only if the potential has an imaginary part.

The condition on $\mathfrak{F}_L$ at the nuclear surface in Eqs. (4) determines the one-body phase shift K_L:

$$\tan K_L=(\mathfrak{F}_LF_L'-\mathfrak{F}_L'F_L)/(\mathfrak{F}_L'G_L-\mathfrak{F}_LG_L'), \quad (6)$$

where a prime indicates differentiation with respect to ρ. The penetration parameters $\pi_1=f_L^2/\rho$ and $\pi_2=\rho/g_L^2$ and then given by

$$\pi_1=(F_L^2/\rho)/|1-F_LG_L\delta_L-iF_L^2\delta_L|^2, \quad (7)$$
$$\pi_2=1/[(A_L^2/\rho)-\pi_1].$$

The physical implications of the reaction cross section given by Eq. (5) are most easily seen for the special case of vanishingly small absorption. Equation (5) then reduces to one of the OBJ results:

$$\sigma_L=(4\pi Pr_0^3/v)(2L+1)\{(F_L/\rho)^2\langle u_L^2\rangle/[(1-F_LG_L\delta_L)^2+F_L^4\delta_L^2]\}, \quad (8)$$

where

$$\langle u_L\rangle^2=\int_0^{r_0}w_L|u_L|^2dr;\quad \int_0^{r_0}w_L(r)dr=1. \quad (9)$$

The quantity $w_L(r)dr$ is the relative intrinsic probability of inducing the reaction in the interval dr at r. For equal probabilities in equal intervals, $w_L(r)$ reduces to the constant $1/r_0$. It is seen in Eq. (8) that, in the limit of very small absorption, σ_L is a function of real quantities only, proportional to P and containing a resonance denominator. The resonance property, which arises from the junction of the internal and external wave functions at the nuclear surface, is also present in very modified form for the case of nonvanishing P.

Since resonances may be defined in various ways the term 90° resonance will be reserved for describing the condition in which $K_L=90°$. For a 90° resonance, $\mathfrak{F}_L=e^{iK_L}\ (F_L\cos K_L+G_L\ \sin K_L)=iG_L$, $d\mathfrak{F}_L/(\mathfrak{F}_Ldr)=dG_L/(G_Ldr)$ and so $(1-F_LG_L\delta_L)=0$. This condition corresponds to a maximum of σ_{sc}/Λ^2 with respect to variations of K_L, where σ_{sc} denotes the partial elastic scattering cross section. It can be shown with the help of Eqs. (4) that the maximum of the wave function inside the nucleus is not reached at the same energy as the maximum of σ_{sc}/Λ^2. For high barriers, however, σ_{sc}/Λ^2 and $|\mathfrak{F}_L(r_0)|^2$ are nearly proportional to one another.[6]

It is of interest to note that the "no-absorption" formula can be written as

$$\sigma_L=(4\pi Pr_0^3/v)(2L+1)\langle u_L^2\rangle(\pi_1/\rho), \quad (10)$$

where π_1 is the penetration parameter defined by Eqs. (7). If $\langle u_L^2\rangle$ is practically independent of energy then $\sigma\propto\pi_1/E$ for this special case.

In order to apply the one-body formula to study various reactions, the internal potential $V-(i\hbar/2)P$ has been put equal to a constant. The internal radial wave function is then

$$\mathfrak{F}_L(z)=(\pi z/2)^{\frac{1}{2}}J_{L+\frac{1}{2}}(z), \quad (11)$$

where $J_{L+\frac{1}{2}}(z)$ is the Bessel function of half integral order. The derivative, $d\mathfrak{F}_L/dz$, which occurs in δ_L, is evaluated by the well-known recurrence relation;

$$d\mathfrak{F}_L/dz=(L+1)\mathfrak{F}_L/z-\mathfrak{F}_{L+1}=-(L\mathfrak{F}_L)/z+\mathfrak{F}_{L-1}. \quad (12)$$

[16] Feshbach, Peaslee, and Weisskopf, Phys. Rev. **71**, 145 (1947).
[17] Fernbach, Serber, and Taylor, Phys. Rev. **75**, 1352 (1949).

The calculation of the cross section thus reduces to the problem of evaluating the Coulomb and complex Bessel functions at the nuclear radius, r_0. The required separation of $\mathfrak{F}_L(z)$ into real and imaginary parts is effected in principle by expressing $\mathfrak{F}_L(z)$ in terms of the trigonometric and hyperbolic functions. In practice this is quite tedious for $L>0$. Using this separation procedure, OBJ derived the partial cross section for s-waves:

$$\sigma_0=\frac{(2\pi P/v)(sh/k_1'-s/k_0')}{|k'|^2(F_0^2+G_0^2)(ch+c)+k^2(F_0'^2+G_0'^2)(ch-c)-2k(k_0's+k_1'sh)(F_0F_0'+G_0G_0')-2k(k_1's-k_0'sh)}. \tag{13}$$

The abbreviations employed here are listed under Notation and Symbols in the Introduction. It is interesting to note that the Coulomb functions occur in combinations which make the introduction of the phase amplitude variables, A_0 and φ_0, convenient.

For calculational purposes, the partial inelastic cross section is expressed in terms of its real and imaginary parts:

$$\sigma_L=(\Lambda^2/\pi)\frac{(2L+1)(F_L^2/\rho)\,\mathrm{Im}(\rho\delta_L)}{[1-F_LG_L\{\mathrm{Re}(\rho\delta_L)/\rho\}+F_L^2\{\mathrm{Im}(\rho\delta_L)/\rho\}]^2+[F_L^2\,\mathrm{Re}(\rho\delta_L)/\rho+F_LG_L\{\mathrm{Im}(\rho\delta_L)/\rho\}]^2}. \tag{14}$$

V. APPROXIMATIONS TO THE REACTION CROSS-SECTION FORMULA

It was seen in the preceding section that the primary difficulty in obtaining an exact and convenient expression for the one-body cross section was due to the presence of complex Bessel functions in Eq. (14). This difficulty is circumvented in practice by appropriate approximations.

If P is small, for example, the quantity $Y(z)=(zd\mathfrak{F}_L)/(\mathfrak{F}_Ldz)$ can be expanded in a Taylor series about the real point k_0r. Thus,

$$Y(z)=Y(k_0r)+\tfrac{1}{2}i\hbar P\left[\frac{\partial}{\partial(\frac{1}{2}i\hbar P)}Y(z)\right]_{P=0}+\cdots. \tag{15}$$

It is observed that Eq. (15) gives the real and imaginary parts of Y as a sum of even and odd powers of P, respectively.

The differential coefficients in Eq. (15) can be evaluated by a method employed by Breit, Thaxton, and Eisenbud.[18] Their procedure determines the coefficient of $\frac{1}{2}i\hbar P$ to be

$$\left[\frac{\partial}{\partial(\frac{1}{2}i\hbar P)}Y(z)\right]_{P=0}=-[(2\mu r/\hbar^2)/\mathfrak{F}_L^2(k_0r)]\int_0^r\mathfrak{F}_L^2(k_0\xi)d\xi$$
$$=-(\mu r^2/\hbar^2)(1-\mathfrak{F}_{L-1}\mathfrak{F}_{L+1}/\mathfrak{F}_L^2). \tag{16}$$

Coefficients of higher powers of $\frac{1}{2}i\hbar P$ are increasingly difficult to evaluate in closed form.

For P very small it is sufficient to keep only the first two terms in the expansion (15). Substitution of this approximation into Eq. (14) yields the cross-section formula,

$$\sigma_L=(4\pi Pr_0^3/v)\frac{(2L+1)(F_L/\rho)^2\langle u_L^2\rangle}{[1-F_LG_L\delta_L+(P\mu r_0/\hbar)F_L^2\langle u_L^2\rangle]^2+[F_L^2\delta_L+(P\mu r_0/\hbar)F_LG_L\langle u_L^2\rangle]^2}, \tag{17}$$

where $\langle u_L^2\rangle$ is defined by Eq. (9). If the terms in the denominator of Eq. (17) containing P are put equal to zero, the OBJ cross-section formula Eq. (8) for vanishingly small absorption is obtained.

Since the expansion for $Y(z)$ is not convergent for all values of P and the calculation of the higher order differential coefficients is quite tedious, an alternative method has been adopted. In this approach a series expansion of $\mathfrak{F}_L(z)$ is made which converges for all finite values of z, namely,

$$\mathfrak{F}_L(z)=\frac{z^{L+1}}{1\cdot3\cdot5\cdots(2L+1)}\left[1-\frac{z^2}{2(2L+3)}+\frac{z^4}{8(2L+3)(2L+5)}-\frac{z^6}{48(2L+3)(2L+5)(2L+7)}+\cdots\right]$$
$$=\frac{z^{L+1}}{1\cdot3\cdot5\cdots(2L+1)}\Omega_L. \tag{18}$$

The corresponding series for $Y(z)$ may be written in the form

$$Y(z)=-L+\frac{(2L+1)\{1-z^2/[2(2L+1)]+z^4/[8(2L+1)(2L+3)]-\cdots\}}{\Omega_L}, \tag{19}$$

[18] Breit, Thaxton, and Eisenbud, Phys. Rev. **55**, 1018 (1939).

by employment of the recurrence relation (12). It is seen that the series (19) is an even function of z. The identification of the real and imaginary parts of $\Omega_L(z^2)$ is facilitated by defining

$$\mathrm{Re}(z^2)=\alpha=(k_0r)^2;\quad \mathrm{Im}(z^2)=\beta=\mu P/\hbar. \tag{20}$$

The quantity α is therefore the square of the wave number for the nuclear region when $P=0$, and β is proportional to P. One may expand therefore as follows:

$$\Omega_L(\alpha+i\beta)=\sum_0^\infty a_n(\alpha, L)(i\beta)^n;\quad a_0(\alpha, L)=\Omega_L(\alpha), \tag{21}$$

where the zeroth coefficient, $a_0(\alpha, L)$, is given by

$$\begin{aligned}a_0(\alpha, L)&=1-\alpha/[2(2L+3)]+\alpha^2/[8(2L+3)(2L+5)]\\&\quad-\alpha^3/[48(2L+3)(2L+5)(2L+7)]+\cdots\\&=1\cdot3\cdot5\cdots(2L+1)\mathfrak{F}_L(k_0r)/(k_0r)^{L+1}.\end{aligned} \tag{22}$$

The second equality sign in Eq. (22) results from the relation of $\Omega_L(\alpha)$ and the spherical Bessel function of real argument.

The coefficients $a_n(\alpha, L)$ in the series (21) for $\Omega_L(\alpha+i\beta)$ can now be expressed in terms of the real functions $\Omega_{L+n}(\alpha)$ by noting that Eq. (21) can be written in the alternative form,

$$\begin{aligned}\Omega(\alpha+i\beta)&=\Omega(\alpha)+(i\beta)[\partial\Omega_L/\partial(i\beta)]_{\beta=0}\\&\quad+[(i\beta)^2/2!][\partial^2\Omega_L/\partial(i\beta)^2]_{\beta=0}+\cdots\\&=\Omega_L(\alpha)+(i\beta)[\partial\Omega_L(\alpha)/\partial\alpha]\\&\quad+[(i\beta)^2/2!][\partial^2\Omega_L(\alpha)/\partial\alpha^2]+\cdots.\end{aligned} \tag{23}$$

The second equation in (23) is a consequence of the symmetry of Ω_L in α and $i\beta$. Employment of the Bessel function identity,

$$2[d/d(x^2)][J_n(x)/x^n]=-J_{n+1}(x)/x^{n+1}, \tag{24}$$

yields the series,

$$\begin{aligned}\Omega_L(\alpha+i\beta)&=\Omega_L(\alpha)-(i\beta)\Omega_{L+1}(\alpha)/[2(2L+3)]+\cdots\\&\quad+(-i\beta)^n\Omega_{L+n}(\alpha)/[n!2^n(2L+3)\cdots\\&\quad\times(2L+2n+1)]+\cdots.\end{aligned} \tag{25}$$

Since Eq. (19) can be written as

$$Y(z)=-L+[(2L+1)\Omega_{L-1}(\alpha+i\beta)]/\Omega_L(\alpha+i\beta), \tag{26}$$

the series (25) permits the calculation of the change of $Y(z)$ with respect to E, V or P in a straightforward manner. In terms of the $\mathfrak{F}_{L+n}(\alpha)$, Eq. (26) becomes

$$Y(z)=-L+\frac{k_0r[\mathfrak{F}_{L-1}(\alpha)+\cdots\langle(-1)^n(i\beta)^n\mathfrak{F}_{L+n-1}(\alpha)/n!2^n(k_0r)^n\rangle+\cdots]}{[\mathfrak{F}_L(\alpha)+\cdots\langle(-1)^n(i\beta)^n\mathfrak{F}_{L+n}(\alpha)/n!2^n(k_0r)^n\rangle+\cdots]}, \tag{27}$$

with the aid of Eq. (18). The quantity $Y(z)$ is expressed in terms of real Bessel functions by means of Eq. (27) and is much more convenient for numerical work than Eq. (19).

There is a third method for obtaining the real and imaginary parts of $Y(z)$ which utilizes the recurrence relation

$$[Y(z)-(L+1)][Y(z)+(L+1)]=-z^2=-\alpha-i\beta, \tag{28}$$

obtainable with the help of Eq. (12). Separation of Eq. (28) into real and imaginary parts gives

$$\begin{aligned}\mathrm{Re}[Y_{L+1}(z)+L+1]&=-\frac{\alpha[\mathrm{Re}Y_L(z)-(L+1)]+\beta\,\mathrm{Im}Y_L(z)}{[\mathrm{Re}Y_L(z)-(L+1)]^2+[\mathrm{Im}Y_L(z)]^2},\\ \mathrm{Im}Y_{L+1}(z)&=\frac{\alpha\,\mathrm{Im}Y_L(z)-\beta[\mathrm{Re}Y_L(z)-(L+1)]}{[\mathrm{Re}Y_L(z)-(L+1)]^2+[\mathrm{Im}Y_L(z)]^2}.\end{aligned} \tag{29}$$

Since the real and imaginary parts of $Y(z)$ for $L=0$ may be determined by the relation $J_0(z)=\sin z$, which was used to obtain the zeroth partial cross section (13), values of these quantities for $L>0$ are determined by repeated application of Eqs. (29).

There are two objectionable features of the recurrence method (29). First, Eqs. (29) obscure the physical origin of the quantities calculated. In this respect, the series calculation of $\mathfrak{F}_L(z)$ is superior, since the latter shows clearly the dependence of $Y(z)$ on P, V and E, and its rate of change with respect to these parameters. The second objection to the recurrence method is that Eqs. (29) require, for given L, the calculation of all values of $z\mathfrak{F}_{L'}/\mathfrak{F}_{L'}dz$ between $L'=L$ and $L'=0$. Therefore, the chance for errors is correspondingly large, and their detection correspondingly difficult. The recurrence method is most useful when z is so large that the series calculation requires the evaluation of an inconvenient number of terms.

It is of interest now to consider another limiting form of the total reaction cross-section formula (14), namely, the case of very strong absorption, P. The consequences of this condition have been examined by Breit, who derived the result reported below in connection with the present work. The result but not the derivation has been stated in another connection.[8]

For strong absorption the wave function is strongly damped in the nuclear region, since the probability is great that a particle will be absorbed from the beam before penetrating the nucleus appreciably. Since

$$k_1'\approx k_0'\approx[\mu P/2\hbar]^{\frac{1}{2}} \tag{30}$$

for P very large, the real and imaginary parts of z are unbounded as P increases. It is therefore permissible to employ the asymptotic form of $\mathfrak{F}_L$,

$$\mathfrak{F}_L\sim\sin[z-(L\pi/2)]. \tag{31}$$

The function u_L which is normalized to unity at the nuclear radius, r_0, is approximately given by

$$u_L \sim [\sin(z - L\pi/2)]/[\sin(z_0 - L\pi/2)]. \quad (32)$$

Since $\sinh(k_1'r)$ and $\cosh(k_1'r)$ have the common asymptotic form $\exp[k_1'r/2]$, Eq. (32) can be written as

$$u_L \sim \exp\{-k_1'(r_0 - r)\} \exp\{ik_0'(r_0 - r)\}. \quad (33)$$

Thus, the normalized interior solution u_L decays exponentially towards the center of the nucleus as was expected, and is independent of L in the limiting case of strong absorption. In this limit,

$$\rho\delta_L \sim -r(du/udr) \sim ik_0'r - k_1'/r. \quad (34)$$

Substitution of Eq. (34) into the cross-section formula (14) yields

$$\sigma_L \sim (\Lambda^2/\pi) \frac{(2L+1)F_L^2 k_0' r_0/\rho}{[1 + F_L G_L k_1' r_0/\rho + F_L^2 k_0' r_0/\rho]^2 + [F_L G_L k_0' r_0/\rho - F_L^2 k_1' r_0/\rho]^2}. \quad (35)$$

The neglect of unity in the denominator of Eq. (35) and the use of the asymptotic forms in Eq. (30) for k_1' and k_0' give the final result,

$$\sigma_L = 2(2L+1)\Lambda\Lambda_0/A_L^2, \quad (36)$$

where $\Lambda_0 = (\hbar/2\mu P)^{\frac{1}{2}}$. It is seen that the dependence of $\sigma_L v$ in Eq. (36) on the Coulomb functions is the same as that of the "penetration factor" employed by Christy and Latter. The quantity Λ_0 is proportional to the particle wave number in the nuclear region. As $P \to \infty$, $\Lambda_0 \to 0$ and σ_L vanishes. This paradox may be explained as follows: the wave function is so strongly damped by the presence of large P that the probability of finding the particle in the nucleus decreases faster than P increases, causing a decreasing cross section.

The simplicity of the result owes its origin to the fact that the wave function decreases at the surface of the nucleus in a thin layer. Within the layer which forms a kind of a skin around the body of the nucleus, the decay of the wave amplitude is given by a simple exponential function provided the skin thickness is small in comparison with the nuclear radius. This situation is very similar to that arising in the familiar case of "skin effect" for high frequency electric currents. Here also the case of small skin thickness gives an especially simple answer.

TABLE II. Values of the depth of the potential well.[a]

Target nucleus	A	B
1. Incident protons		
Li^7	40.00	31.7
C^{12}	17.6	11.06
O^{16}	13.4	8.07
Na^{23}	21.00	16.79
Si^{28}	10.86	7.73
2. Incident alpha-particles		
Target nucleus	A	B
He^4	10.0	5.80
Li^6	11.55	8.55
Be^8	13.10	10.71
B^{11}	15.48	13.61
C^{12}	11.40	9.63
N^{14}	8.13	6.56
O^{16}	8.17	6.75
F^{19}	14.38	13.12

[a] The symbol A indicates that the radius is $1.6 \times 10^{-13} A^{\frac{1}{3}}$ cm. The symbol B indicates that the radius is $2.1 \times 10^{-13} A^{\frac{1}{3}}$ cm.

VI. CROSS SECTIONS FOR VANISHINGLY SMALL ABSORPTION

It was seen in Secs. IV and V that the one-body model gives a formula for the reaction cross section which admits factorization in terms of a penetration parameter only in certain limiting cases. In this section the one-body cross section without absorption, Eq. (8), is applied to the study of some of the reactions listed in Sec. III.

For the rectangular well, Eq. (9) becomes

$$\langle u_L^2 \rangle = (1/r_0) \int_0^{r_0} u_L^2 dr = (1 - \mathfrak{F}_{L-1}\mathfrak{F}_{L+1}/\mathfrak{F}_L^2)/2, \quad (37)$$

where $\mathfrak{F}_L$ is a function of the real argument $k_0 r_0$, and is related to the Bessel function $J_{L+\frac{1}{2}}(k_0 r_0)$ by

$$\mathfrak{F}_L = (\pi k_0 r_0/2) J_{L+\frac{1}{2}}. \quad (38)$$

Since the depth $U = |V|$ of the one-body well is subject to considerable uncertainty, several values of U, in conjunction with the two nuclear radii selected in III, have been employed. These are designated the binding energy,[19] "zero," and special Van Vleck[20] well depths, respectively. As the name implies, the second named well depth simply corresponds to the case $U = 0$. The special Van Vleck well depth is the ordinary Van Vleck well depth evaluated for zero bombarding energy. This device removes the small velocity dependence of the latter well. The values of the binding energy well depth are listed in Table II.

For small values of P it is convenient to make use of Eq. (8) and to tabulate the quantity $\sigma_L v/(2\pi P)$. This procedure leaves the absolute magnitude of the cross section unspecified, but permits comparisons of the yield curves for different assumptions about the potential well. The factor $v/2\pi$ has been inserted in order to deal directly with a quantity proportional to the number of incident particles inside the nucleus, for a unit flux of incident particles.

In order to show details of the cross section away from resonance, a logarithmic scale was adopted for $\sigma_L v/2\pi P$. For proton bombardment, the quantity

[19] See Appendix.

[20] J. H. Van Vleck, Phys. Rev. 48, 467 (1935); Ostrofsky, Bleick, and Breit, Phys. Rev. 49, 352 (1936). See Appendix.

$\mathfrak{L}=\log_{10}[(\sigma_L v/2\pi P)\times 10^{39}\ \text{cm}^3]$ was plotted against $E_{\text{Mev}}^{-\frac{1}{2}}$, and, for alpha-particles, $\mathfrak{L}$ was plotted against E_{Mev}.

If $\delta_L=0$ and $\langle u_L^2\rangle=\frac{1}{2}$ in Eq. (8), then $\sigma_L v/2\pi P=(2L+1)r_0^2(F_L/\rho)^2$. The quantity on the right side, which is proportional to Π_1/ρ and has the same low energy dependence as $\sigma_L v$ in Eq. (8), namely, $\sigma_L v \propto e^{-2\pi\eta}/v$. It may be used as a "penetration factor" measure of the one-body cross section, but it is seen that the only justification for such a terminology is in the relation of the "penetration factor" to $\sigma_L v$.

Some[12] representative results are displayed in Figs. 3–5. Comparison of the $\mathfrak{L}$ and $\mathcal{P}=\log_{10}[(2L+1)r_0^2\times(F_L/\rho)^2 10^{39}\ \text{cm}^3]$ curves in Figs. 3 and 4 show that their large structural differences are by no means localized in the immediate vicinity of the one-body resonances. These differences persist both above and below resonance. Both $\mathfrak{L}$ and $\mathcal{P}$, however, show the same rapid increase in the low energy region as E_{Mev} increases, since the major energy dependence here is due to the factor $(F_L/\rho)^2$.

Many of the calculated one-body cross sections exhibited no resonance in the energy interval plotted. The presence of a resonance just outside the interval however, decidedly altered the shape of $\mathfrak{L}$ in comparison with $\mathcal{P}$. As has been shown by OBJ, conclusions drawn from fitting nonresonant excitation functions to various

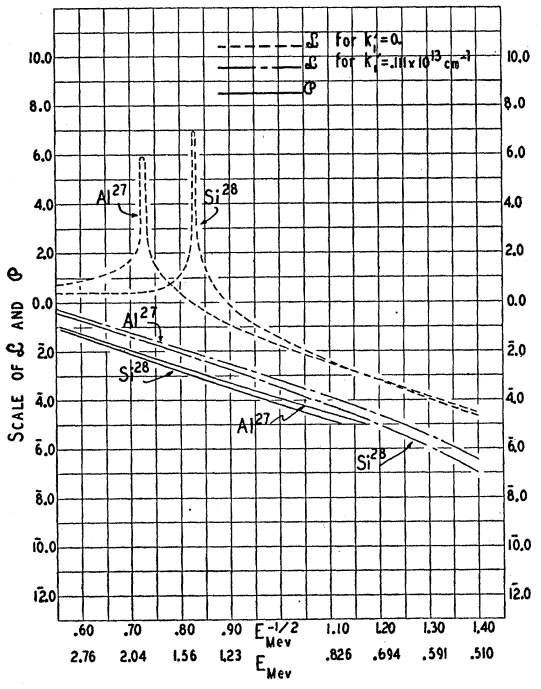

FIG. 3. One-body cross sections for $Al^{27}(p,\ )$ and $Si^{28}(p,\ )$, compared with a "penetration factor" cross section. Dashed lines: $\mathfrak{L}$ *vs* $(E_{\text{Mev}})^{-\frac{1}{2}}$ for $k_1'=0$; long-short dashed lines: $\mathfrak{L}$ *vs* $(E_{\text{Mev}})^{-\frac{1}{2}}$ for $k_1'=0.111\times10^{13}\ \text{cm}^{-1}$; solid lines: $\mathcal{P}$ *vs* $(E_{\text{Mev}})^{-\frac{1}{2}}$. All curves were computed for $L=3$, $U=28.63$ Mev, and $r_0=1.6\times10^{-13}A^{\frac{1}{3}}$cm.

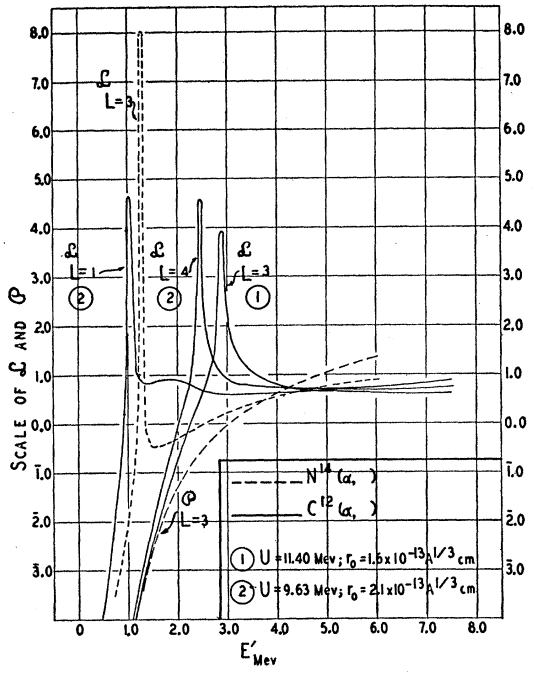

FIG. 4. The "no-absorption" cross sections for $N^{14}(\alpha,\ )$ and $C^{12}(\alpha,\ )$. Dashed curves: $\mathfrak{L}$ *vs* $(E_{\text{Mev}}')^{-\frac{1}{2}}$ and $\mathcal{P}$ *vs* $(E'_{\text{Mev}})^{-\frac{1}{2}}$ for the reaction $N^{14}(\alpha,\ )$ with $r_0=2.1\times10^{-13}A^{\frac{1}{3}}$ cm and $U=6.56$ Mev. Solid curves: $\mathfrak{L}$ *vs* $(E_{\text{Mev}}')^{-\frac{1}{2}}$ for $C^{12}(\alpha,\ )$ with parameters as stated. For $N^{14}(\alpha,\ )$, $E_{\text{Mev}}'=(7/9)E_{\text{Mev}}$; for $C^{12}(\alpha,\ )$, $E_{\text{Mev}}'=(3/4)E_{\text{Mev}}$.

"penetration factors" may diverge widely from those deduced from a potential well calculation.

The regularities, as a function of the atomic number, which appeared in the penetration parameter curves of Sec. III should be absent in the reaction cross sections computed with the binding energy well depths since the latter are not smooth functions of Z'. For the special Van Vleck and zero well depths, however, these regularities should persist since these well depths are independent of Z'. This expectation is confirmed in Fig. 4 for the triad C^{12}, N^{14}, and O^{16} under proton bombardment and with the two special Van Vleck well depths corresponding to the two choices of radius. It is seen that the energy of a particular resonance decreases as Z' increases. The relatively depressed values of $\mathfrak{L}$ for Si^{28} at low energies are effected by the Coulomb barrier.

An apparent difficulty in evaluating the cross-sectional formula (8) occurs when the quantity δ_L becomes infinite. This situation arose in the course of the calculations whenever $\mathfrak{F}_L$ vanished. The vanishing of $\mathfrak{F}_L$ causes no anomaly in the cross section, however, as the following argument shows.

If in Eq. (8) $\mathfrak{F}_L$ approaches zero, then δ_L becomes very large, and so unity can be neglected in comparison with $F_L G_L \delta_L$ in the denominator. The resulting partial cross section is then

$$\sigma_L=(4\pi P r_0^2/v)(2L+1)\langle u_L^2\rangle/(\rho A_L \delta_L)^2. \qquad (39)$$

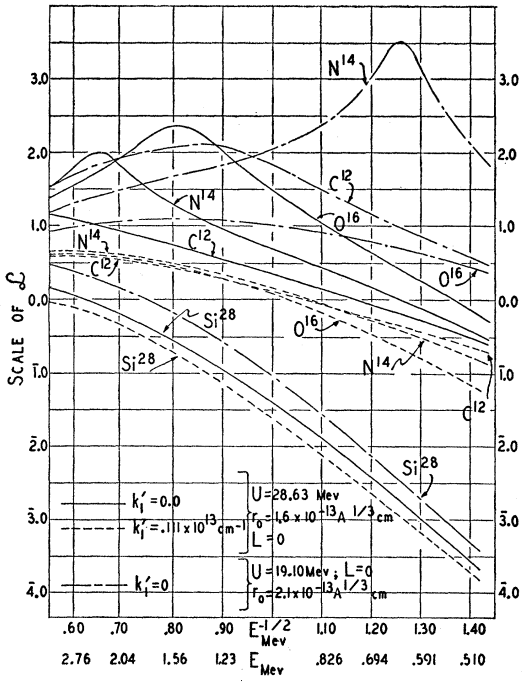

FIG. 5. One-body reaction cross sections for $N^{14}(p,\ )$, $O^{16}(p,\ )$, $Si^{28}(p,\ )$, and $C^{12}(p,\ )$. Solid lines: $\mathfrak{L}$ *vs* $(E_{\text{Mev}})^{-\frac{1}{2}}$ for $U=28.63$ Mev, $r_0=1.6\times10^{-13}A^{\frac{1}{3}}$ cm, and $k_1'=0$; Long-short dashed lines: $\mathfrak{L}$ *vs* $(E_{\text{Mev}})^{-\frac{1}{2}}$ for $U=19.10$ Mev, $r_0=2.1\times10^{-13}A^{\frac{1}{3}}$ cm, and $k_1'=0$; Dashed lines: $\mathfrak{L}$ *vs* $(E_{\text{Mev}})^{-\frac{1}{2}}$ for $U=28.63$ Mev, $r_0=1.6\times10^{-13}A^{\frac{1}{3}}$ cm and $k_1'=0.111\times10^{13}$ cm^{-1}. For all curves, $L=0$.

If the terms in Eq. (39) not containing $(\mathfrak{F}_L)^{-1}$ are neglected, Eq. (39) can be written as

$$\sigma_L\approx-(2\pi Pr_0^3/v)(2L+1)\mathfrak{F}_{L+1}/[(k_0r_0)^2A_L^2\mathfrak{F}_{L-1}]. \quad (40)$$

with the aid of Eq. (37). Hence, the cross section is finite and changes smoothly in the neighborhood of a zero of $\mathfrak{F}_L$.

The analysis of the $Li^7(p,\alpha)\alpha$ reaction illustrates some of the limitations of the one-body model. The yield[21] of this reaction exhibits a broad maximum at $E=3$ Mev and theoretical fits[15] to the angular distribution ascribe this condition to two levels of the compound nucleus Be^8. The first level, approximately 1 Mev wide, occurs at $E=3$ Mev with $I=2$ and even parity; the second level, approximately centered on 3 Mev, with a width of several Mev, is supposed to have $I=0$ and even parity, and be excited by both p and f protons.

In Fig. 6 the behavior of the one-body cross section for the $Li^7(p,\alpha)\alpha$ reaction is shown. The well depth, $U=19.52$ Mev, was chosen to give a resonance of σ_1 at about 3 Mev. It should be noted that the quantity plotted, $\mathfrak{L}$, is a function of $\sigma_1 v$. With the other parameters equal to those of Fig. 6, the value $U=18.6$ Mev satisfies the 90° resonance condition at $E=3$ Mev. But the maximum of σ_1 is then shifted up to about $E=3.2$ Mev.

No attempt is being made here to consider the effect of different relative spin orientations. Such considerations can presumably be carried out best in the framework of a "dispersion theory" representation. The problem has been considered from this viewpoint by Inglis *et al.*[15] On the other hand, calculations of the present paper show that the experimental resonance is much narrower than that indicated by the "one-body" treatment as would be expected on most theories of many-body effects.

The logarithms of the penetration parameters $\pi_1=f_L^2/\rho$ and $\pi_2=\rho/g_L^2$ for the $Li^7(p,\ )$ reaction have also been plotted in Fig. 6. Comparison of the $\mathfrak{L}$ and $\mathfrak{l}_1=\log_{10}\pi_1$ curves shows that they have similar shapes, but that the maximum value of $\mathfrak{l}_1$ occurs at a slightly higher energy. This shift is due to the energy dependence of the factor $\langle u_L^2\rangle/\rho$ in Eq. (10), which is important for a broad resonance. In this quantity in the present case the factor $1/\rho$ accounts for most of the variation as E is varied from 1 to 2 Mev. But for a sharp resonance $\mathfrak{L}$ and $\mathfrak{l}_1$ will be similar functions of energy, with their maxima occurring for the same value of E. Away from resonance the factor F_L^2/ρ in $\mathfrak{L}$ and $\mathfrak{l}_1$ contains the principal energy dependence of these two functions. The reason for the presence of the sharp maximum in the $\mathfrak{l}_2=\log_{10}\pi_2$ function can be seen with the help of Eqs. (7) which define the barrier parameters π_1 and π_2

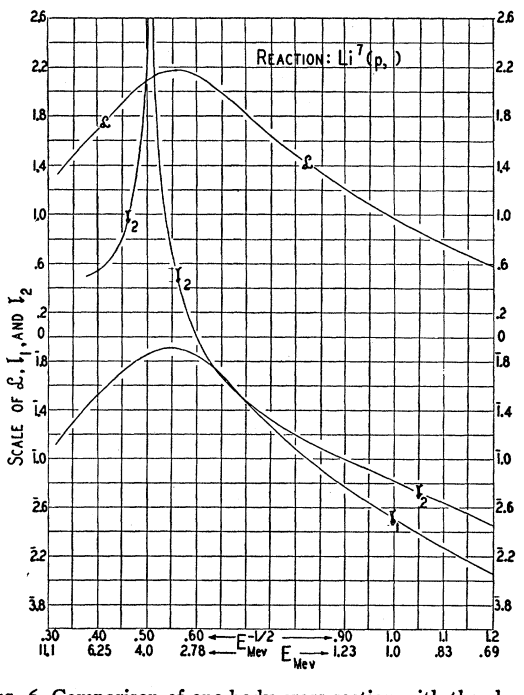

FIG. 6. Comparison of one-body cross section with the channel penetration parameters for $Li^7(p,\ )$: $\mathfrak{L}$, $\mathfrak{l}_1$ $\mathfrak{l}_2$ *vs* $E_{\text{Mev}}^{-\frac{1}{2}}$; $\mathfrak{l}_1$ and $\mathfrak{l}_2$ were normalized at 2.04 Mev. $L=1$ and $r_0=1.6\times10^{-13}A^{\frac{1}{3}}$ cm. The well depth $U=19.52$ Mev was chosen to give a one-body resonance at about 3 Mev.

[21] Hornyak, Lauritsen, Morrison, and Fowler, Revs. Modern Phys. 22, 291 (1950).

in terms of the one-body model. Since $f_L^2+g_L^2=A_L^2$, π_1 always must satisfy the condition $\pi_1 \leq A_L^2/\rho$, the case of equality representing a singular point of π_2. For a broad, flat resonance π_1 varies slowly over a wide range of energy values, while A_L^2/ρ decreases rapidly as E increases from 0. These circumstances provide an opportunity for A_L^2/ρ to "catch up" with π_1, as is exemplified by Γ_2 in Fig. 6. The singular point of Γ_2, i.e., the point at which $A_L^2=\pi_1$, cannot occur on the low energy side of the resonance of Γ_1 in Fig. 6 because the quantity A_L^2/ρ is decreasing monotonically as E increases.

The half-widths of the one-body resonances depend strongly on the energy and angular momentum for which they occur. In general, the half-width decreases with increasing angular momentum and decreasing energy. To obtain a quantitative estimate of this dependence, the half-widths were calculated from the curves by treating the resonances in a way similar to that of Breit and Yost.[22]

The one-level dispersion formula near sharp resonance suggests that the partial cross section may be written as

$$\sigma_L = A/[(E-E_0)^2+B], \tag{41}$$

where A and B are almost constant functions of E in the vicinity of resonance, and E_0 is the energy at which the resonance peak occurs. Since the quantity $(1-F_LG_L\delta_L)$ is very nearly a linear function of energy in the range of interest, it is assumed that it can be approximated near E_0 in the form $C(E-E_0)$, where C is energy independent. The quantity B is identified as $(F_L^2\delta_L/C)^2$ by comparison with (8). The value of $E-E_0=\Delta E$ for which Eq. (8) has a value equal to one-half of the maximum value, A/B, is given by $\Delta E=\pm|B|^{\frac{1}{2}}$, so that the width at half-maximum is $2\Gamma=2|B|^{\frac{1}{2}}$.

The values of $F_L^2\delta_L$ and C at $E=E_0$ have been calculated for a number of resonances together with the corresponding half-widths; some of the results are listed in Table III. The table illustrates the rapid decrease in the half-width for decreasing energy and increasing angular momentum. It should be noted that in the transition from a one-body resonance to the corresponding many-body resonance, the resonance may be sharpened appreciably.

The principal energy dependence in the expression for the half-width is contained in the factor F_L^2. The maximum variation of C is roughly an order of magnitude, while the quantity δ_L at resonance varies by only a factor of four or five at most. These circumstances provide a convenient method for investigating the energy dependence of the half-width: for a particular element, small changes in the depth of the potential well are made, thus shifting the resonance peak. Since only small variations in δ_L and C result from the altered well depths, a constant factor times F_L^2 yields a qualitative estimate

[22] G. Breit and F. L. Yost, Phys. Rev. **48**, 204 (1935).

TABLE III. Half-widths of resonances for incident protons.[a]

Isotope	r_0	L	U(Mev)	E_0(Mev)	2Γ(Mev)
N^{14}	A	2	28.63	0.67	0.0006
C^{12}	A	2	28.63	2.75	0.3
Be^{9}	B	2	19.10	2.6	0.5
B^{11}	B	2	19.10	0.83	0.01
Al^{27}	A	3	28.63	1.9	0.002
Si^{28}	A	3	28.63	1.45	0.0002
F^{19}	B	3	19.10	2.7	0.08
Na^{23}	B	3	19.10	0.85	0.00006
Al^{27}	B	1	19.10	2.00	0.4
Si^{28}	B	1	19.10	1.72	0.1
Ne^{20}	B	0	0.00	2.20	2
Mg^{24}	B	0	0.00	2.10	1
Al^{27}	B	0	0.00	2.04	0.7
Si^{28}	B	0	0.00	2.10	0.6

[a] The symbol A indicates the radius is $1.6\times10^{-13}A^{\frac{1}{3}}$ cm. The symbol B indicates the radius is $2.1\times10^{-13}A^{\frac{1}{3}}$ cm.

of the dependence of the half-width on energy. The behavior of the one-body cross section as a function of well depth for constant energy of relative motion is shown in Fig. 7 for the $B^{11}(\alpha,)$ reaction.

Another interesting feature is the dependence of the resonance height on energy. At a 90° resonance, the partial cross section is given by

$$(\sigma_L)_{\text{res}} = (4\pi Pr_0^3/v)(2L+1)\langle u_L^2\rangle/(\rho F_L\delta_L)^2. \tag{42}$$

Since the half-width is given by $2|F_L^2\delta_L/C|$, it can be concluded that the area under the resonance curve is roughly constant, i.e., independent of the energy at which the peak is located.

The occurrence of F_L^2 in the expression for the half-width indicates that the penetration parameter containing F_L^2 is in some degree applicable to this model. The assumptions which led to this identification were that: (1) the resonance is sharp, (2) the quantity $(1-F_LG_L\delta_L)$ is a linear function of the energy in the resonance region, and (3) δ_L is a constant near resonance. These approximations are not completely valid, but, in many cases, the penetration parameter Π_1 should suffice in getting orders of magnitude.

Figure 8 consists of contour plots of the cross section as a function of bombarding energy and well depth for the $C^{12}(p,)$ reaction. These curves confirm the expectation that increasing the depth of the potential well decreases the energy at which the resonance occurs, and indicate how the shape of the resonance peak depends on its energy level.

A single resonance is represented by a contour ridge —a line of slowest descent—running approximately along the $E+U=$ const line[23] in the (U, E) plane, since k_0 and, hence, $d\mathfrak{F}_L/[\mathfrak{F}_L d(k_0r_0)]$ are constant along this line. Near resonance the latter quantity is by far the most rapidly varying function of energy in the expression $(1-F_LG_L\delta_L)$, which itself varies slowly with energy in the region of resonance.

In the limit of zero energy the cross section contains

[23] It should be noted that the horizontal and vertical scales in Figs. 8 and 9 are unequal.

singularities along the U axis. As is expected, however, these singular points are removed by the introduction of a finite damping coefficient.

VII. EFFECT OF ABSORPTION ON THE CROSS SECTION

Within the limitations of the one-body model, the results presented in the preceding section should be valid whenever the inelastic cross section of a scattering process is small. But, for reactions of high yield, formula (8) is not applicable. The partial cross section σ_L is no longer proportional to the imaginary part of the potential, but, as a function of P, reaches a maximum and finally decreases to zero as P becomes very large.

For finite absorption the sharp resonances which were prominent features of the "no-absorption" calculations are modified appreciably. This modification of the resonance shapes and the variation of the cross section with P have been investigated for some of the reactions of Sec. VI with the aid of the general one-body formula (14) for the reaction cross section. The lengthy calculations required to evaluate Eq. (14) restricted the scope of this study. For the case of incident protons with the special Van Vleck interaction, reaction cross sections have been computed for the isotopes C^{12}, N^{14}, O^{16}, Al^{27} and Si^{28}, employing $L=0$, 1, 2, 3, 4 and $r_0=1.6\times10^{-13}A^{\frac{1}{3}}$ cm; and the isotopes Be^9, B^{11}, C^{12}, N^{14}, F^{19}, Na^{23}, Al^{27} and Si^{28} with $r_0=2.1\times10^{-13}A^{\frac{1}{3}}$ cm and the same range of L. In addition, the $B^{11}(\alpha,\ )$ reaction was investigated for various combinations of U, r_0, and L.

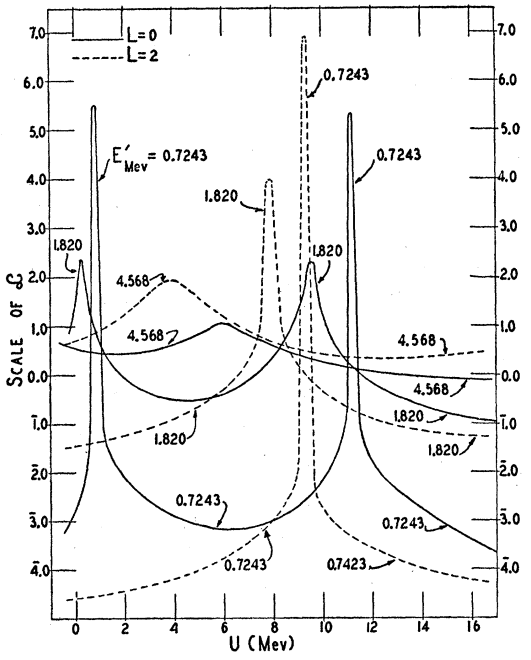

FIG. 7. Resonances of the cross section for $B^{11}(\alpha,\ )$ as a function of the well depth U at a constant energy of relative motion E_{Mev}'. Each curve is a plot of $\mathfrak{L}$ *vs* U for the constant values of L and E_{Mev}' shown. For all curves, $r_0=1.6\times10^{-13}A^{\frac{1}{3}}$ cm. $E_{\text{Mev}}'=0.733E_{\text{Mev}}$.

The absorption coefficient used in the evaluation of Eq. (14) was obtained from Fernbach, Serber and Taylor's[17] analysis of total cross sections of nuclei to high energy neutrons. The value which has been found is $k_1'=0.111\times10^{13}$ cm^{-1}.

Two methods have been used to calculate the real and imaginary parts of $(zd\mathfrak{F}_L)/(\mathfrak{F}_L dz)$ which appear in Eq. (14). The major portion of the calculations was performed using Eq. (27) of Sec. V. This method gave values to three significant figures with the neglect of all terms beyond the fourth or fifth in the series defined by Eq. (27). The other method utilized the recurrence relation for the Bessel function as given by Eqs. (29).

Some[12] results of these calculations, shown in Figs. 3 and 5, are compared directly with the corresponding "no-absorption" curves. It is seen in Fig. 3 that the introduction of absorption drastically modifies the sharp resonances which occur for large L in the "no-absorption" case.

The contours of the quantity $\mathfrak{L}$ for the $C^{12}(p,\ )$ reaction with absorption are shown in Fig. 9. It is seen that the cross section now goes to zero at $E=0$, in contrast to the case of "no-absorption" in Fig. 8. In fact, the introduction of absorption modifies the contour ridges to such an extent that, for $L>0$, the cross section does not increase at all with decreasing E. For $L=0$ the cross section rises to a peak value—a maximum of a function of two variables—the location of the peak being at $E\approx2.2$ Mev, $U=2.0$ Mev.

The variation of $\mathfrak{L}$ with k_1' is illustrated in Fig. 10 for the $O^{16}(p,\ )$ reaction. It is seen that increasing k_1' decreases the maximum and increases the half-width of the resonance. Since this effect is very pronounced even for small values of k_1', the resonance peak is barely detectable when k_1' has increased to the Serber value, $k_1'=0.111\times10^{13}$ cm^{-1}. Nevertheless, the resonance may still be identified by noting the steeper slope on the low energy side of the resonance "peak," and the more gentle slope on the high energy side in comparison with the case of no resonance. Thus, the cross section is greater than its value would be if there were no resonance in the energy interval considered.

VIII. SUMMARY

In the energy interval from 0.5 to 3.0 Mev it was noted that the principal deviation in the energy dependences of the penetration parameters F_L^2/ρ and ρ/G_L^2 occurred for $L=0$, and that this deviation almost vanished for large L. This situation is illustrated in Fig. 1 for the $Li^7(p,\ )$ reaction. The difference, $\log_{10}(\rho/G_0^2)-\log_{10}(F_0^2/\rho)$, of the curves for $L=0$ passes through a sequence of values from 0.112 to -0.106 and then rises to zero as E increases to 3 Mev. The absolute change of this difference over the whole energy interval is 0.149 for $L=1$ and only 0.007 for $L=4$, so that the

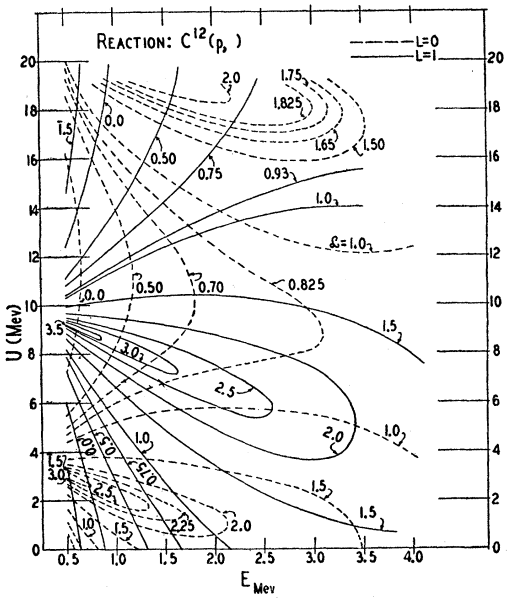

FIG. 8. Contours in the (U, E_{Mev}) plane of the reaction cross section for $C^{12}(p,)$ with $k_1'=0$. The curves are plots of U *vs* E_{Mev} for the constant value of $\mathfrak{L}$ shown; $r_0=2.1\times10^{-13}A^{\frac{1}{3}}$ cm.

cumulative correction to the almost constant ratio of the penetration parameters is a factor of 1.41 in the former case, and 1.02 in the latter. In Fig. 2 the comparison of the logarithms of the penetration parameters is carried out over an extended energy scale for $L=1$. With the curves fitted at 0.5 Mev, their difference slowly increases with E and reaches a maximum of about 0.226 near the height of the potential barrier. The difference then decreases with the indication of a second intersection of the curves beyond the high energy side of the scale. Table I shows the closely parallel behavior of the parameters ρ/G_L^2 and ρ/A_L^2 in regions where the barrier is high.

The OBJ one-body model was used to test the reliability of these parameters in representing barrier penetration effects, and special limiting cases, in which the barrier dependence of the resonance half widths could be identified as "penetration factors," were discussed. In particular it was shown that the penetration parameter ρ/A_L^2 could be identified with the case of very strong absorption of the incident wave. Figures 3, 4, and 5 present a selection of one-body cross sections with and without absorption, compared in certain cases with a "penetration factor" derived from the one-body model. Figures 4 and 5 indicate how the potential well can drastically modify the energy dependence of the yield expected from a "penetration factor" analysis, even at energies considerably removed from the virtual resonance level. Figures 3 and 5 show the effect that absorption has on the one-body cross sections. The absorption coefficient, k_1', which was derived from the analysis of high energy scattering data, is so large that the resonance features of the "no-absorption" model are practically obliterated. In Fig. 6 the channel penetration parameters, f_L^2/ρ and ρ/g_L^2, are applied to the study of the $Li^7(p,)$ reaction, and compared with the OBJ cross section without absorption. For a sharp resonance it was seen that f_L^2/ρ is by far the major energy dependent factor in the one-body cross section formula, and, thus, in this case the barrier dependence of the damping constant is not separable from purely nuclear effects. Figures 7, 8, and 9 illustrate how the one-body resonances depend on the parameters which describe the compound nucleus, namely, the nuclear radius, well depth, bombarding energy, angular momentum, and absorption coefficient. The $O^{16}(p,)$ reaction in Fig. 10 has been selected to investigate the variation of the cross section as a function of the absorption coefficient.

The many body features of nuclear reactions are included in the present study only to the degree of taking into account schematically the absorption of the incident wave in nuclear matter.

We are greatly indebted to Professor G. Breit who initiated and guided this work. In particular, we wish to thank him for supplying us with the result for the case of very strong absorption. To Professor Breit and Professor C. Kittel, we extend our thanks for the use of some unpublished work which influenced the course of the present calculations.

We are grateful to Mr. Harrison M. Jones and Mr. John L. Johnson for their help in various phases of this work. Mr. Johnson has in addition read the manuscript

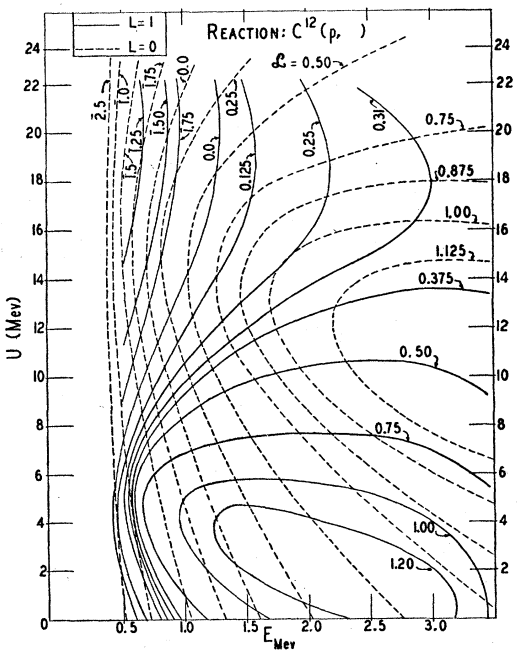

FIG. 9. Contours in the (U, E_{Mev}) plane of the reaction cross section with absorption for $C^{12}(p,)$. The curves are plots of U *vs* E_{Mev} for the constant value of $\mathfrak{L}$ shown. For all curves, $k_1'=0.111\times10^{13}$ cm^{-1}, and $r_0=1.6\times10^{-13}A^{\frac{1}{3}}$ cm.

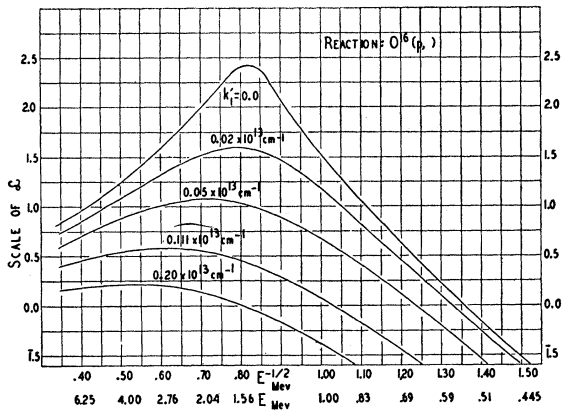

FIG. 10. Effect of absorption on the one-body resonance of $O^{16}(p,\ )$: $\mathfrak{L}$ *vs* $E_{\text{Mev}}^{-\frac{1}{2}}$ for constant k_1'. For all curves $U=28.63$ Mev, $r_0=1.6\times10^{-13}A^{\frac{1}{3}}$ cm, and $L=0$.

critically, and checked the formulas. We also wish to thank Mr. James F. Bartram, Mrs. Martha C. Meeker, Mrs. Carolyn Arfken, Mrs. Dorothea Bone, and Miss Jacqueline Gibson for assistance with the calculations and preparation of the figures.

APPENDIX

1. *Binding energy well depth:* This estimate is provided by the binding energy of the incident particle in the compound nucleus. The kinetic energy in the ground state of the last bound particle is estimated by assuming that r times the radial wave function is a sine wave which vanishes at the nuclear boundary. Large binding energies and large extra-nuclear Coulomb barriers suppress the tail of the wave function and hence, improve the approximation. For these assumptions the well depth is related to the binding energy by $U=B+(\hbar\pi)^2/(2\mu r_0^2)$, where B is the absolute value of the binding energy, and the second term on the right is the ground state kinetic energy. The well depth computed from this formula, using the correct binding energy, may be much too small for the heavier elements because of the action of the exclusion principle in requiring the last bound particle to occupy an excited state.

2. *Van Vleck well depth:* Van Vleck considered the case of incident neutrons, and Ostrofsky, Bleick, and Breit made application to the case of incident protons. It was assumed by Van Vleck that the interaction between all pairs of nucleons is of the Majorana exchange type, and that the nucleons are distributed according to the Thomas-Fermi statistical model. Additional approximations similar to those made in the Hartree-Fock treatment are also required. Surface effects are eliminated by assuming that the range of the force is small compared with the nuclear radius. The well depth resulting from this calculation depends slightly on the energy of the incident particle. In the present application the velocity dependence has been neglected, and the depth at zero energy used. The latter well depth is called the special Van Vleck well depth in the text.

The Van Vleck formula for the potential well is

$$V=-A\{E(W_+)\mp E(W_-)+2[\alpha/(\pi k_P^2)]^{\frac{1}{2}}[e^{-W_+^2}-e^{-W_-^2}]\},$$

where the sign is negative if $k_P>k$, and positive if $k_P<k$. Here,

$$W_\pm=|k_P\pm k|/(2\alpha^{\frac{1}{2}});\quad E(W)=(2\pi^{-\frac{1}{2}})\int_0^W e^{-t^2}dt;$$

and

$$k=[(9\pi N)/(4r_0^3)]^{\frac{1}{3}}$$

with N equal to the number of neutrons; k_P is 2π times the wave number of the proton inside the nucleus and the neutron-proton potential is $Ae^{-\alpha r^2}$. In order to evaluate V from the above formula, a method of successive approximations was used. The value of N was placed equal to one-half of the mass number, so that with the radius convention employed in Sec. III, k and V become independent of target element. Use of the values obtained from proton-proton scattering, $\alpha=1.23\times10^{24}$ cm^{-2} and $A=100$ Mev, determined the value of the Van Vleck well depth at zero bombarding energy as follows:

$$V=-28.63 \text{ Mev} \quad \text{for} \quad r_0=1.6\times10^{-13}A^{\frac{1}{3}} \text{ cm},$$

and

$$V=-19.10 \text{ Mev} \quad \text{for} \quad r_0=2.1\times10^{-13}A^{\frac{1}{3}} \text{ cm}.$$